PCCP

Physical Chemistry Chemical Physics

www.rsc.org/pccp

Volume 15 | Number 44 | 28 November 2013 | Pages 19075–19520

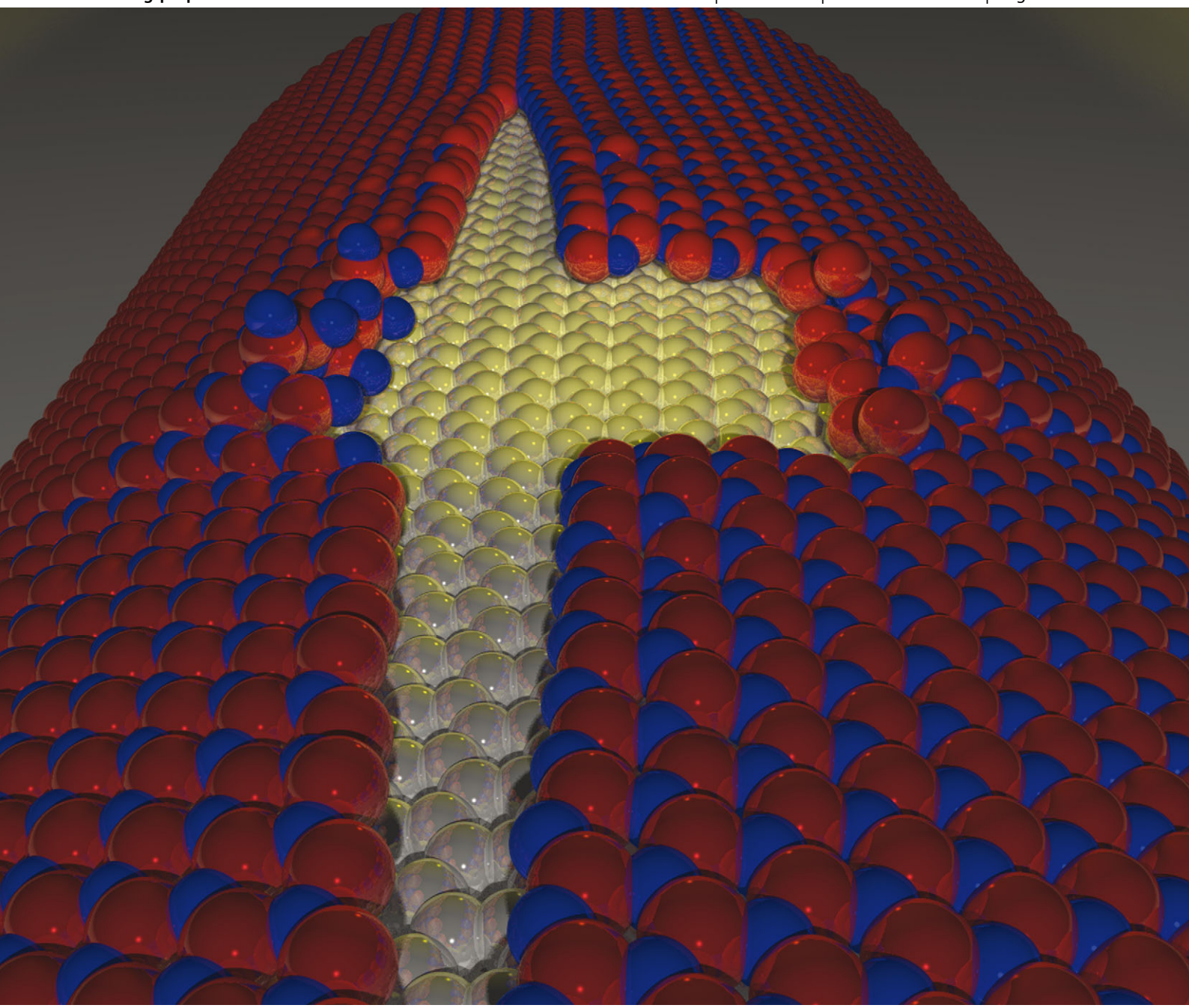

ISSN 1463-9076

PAPER

Paupitz *et al.*

Dynamical aspects of the unzipping of multiwalled boron nitride nanotubes

1463-9076(2013)15:44;1-I

PCCP

RSC Publishing

PAPER

View Article Online
View Journal | View Issue

Cite this: *Phys. Chem. Chem. Phys.*, 2013, **15**, 19147

Dynamical aspects of the unzipping of multiwalled boron nitride nanotubes†

E. Perim,[a] P. A. S. Autreto,[a] R. Paupitz*[b] and D. S. Galvao[a]

Received 27th June 2013,
Accepted 7th August 2013

DOI: 10.1039/c3cp52701h

www.rsc.org/pccp

Boron nitride nanoribbons (BNNRs) exhibit very interesting magnetic properties, which could be very useful in the development of spintronic based devices. One possible route to obtain BNNRs is through the unzipping of boron nitride nanotubes (BNNTs), which have been already experimentally realized. In this work, different aspects of the unzipping process of BNNTs were investigated through fully atomistic molecular dynamics simulations using a classical reactive force field (ReaxFF). We investigated multiwalled BNNTs of different diameters and chiralities. Our results show that chirality plays a very important role in the unzipping process, as well as the interlayer coupling. These combined aspects significantly change the fracturing patterns and several other features of the unzipping processes in comparison to the ones observed for carbon nanotubes. Also, similar to carbon nanotubes, defective BNNTs can create regions of very high curvature which can act as a path to the unzipping process.

1 Introduction

With the advent of graphene[1] and the revolution in materials science it created, there is renewed interest in other two-dimensional structures.[2–6] Among these structures, one of the most important is hexagonal boron nitride (hBN).[7,8] However, the synthesis of BN structures is in general difficult, and only recently BN monolayers have been obtained.[9–14]

hBN (also known as *white graphite*) is considered the inorganic analogue of graphite.[7] These structures are isoelectronic and share the same hexagonal honeycomb lattice. Indeed, there are corresponding BN structures to carbon-based graphene, fullerenes and nanotubes. Even the BN equivalent to carbon nanoscrolls, which was theoretically predicted,[15] has been recently experimentally realized.[16,17]

Another important family of structures directly related to graphene and BN monolayers are the so-called nanoribbons (molecular fragments with a large aspect ratio). Carbon nanoribbons (CNRs) present interesting electronic properties.[18] Similarly, BN nanoribbons (BNNRs) are predicted to also present interesting electronic properties,[19,20] in particular, magnetic ones to be exploited in the development of spintronic devices.[20–25]

The unzipping of carbon nanotubes is one of the most promising ways of producing CNRs. Different chemical and physical methods have been successfully used to achieve this.[18,26,27] In principle, the same approaches could be used to produce BNNRs from the unzipping of BN nanotubes (BNNTs). However, due to experimental difficulties, there are only a few studies reporting the BNNR production.[12,28] In one experiment,[12] plasma etching was used to produce the unzipping of BNNTs, yielding good quality BNNRs, while in the other,[28] BNNTs were intercalated with potassium leading to the fracturing (unzipping) process, which also resulted in good quality BNNRs. However, some of the dynamical aspects of these processes are not yet fully understood.

2 Methodology

In order to gain further insights into the dynamics of the BNNT unzipping, we have carried out fully atomistic molecular dynamics simulations using the reactive force field ReaxFF,[29] as implemented in the LAMMPS package.[30]

ReaxFF is parametrized using DFT calculations and employs a bond length–bond order relationship, allowing the simulation of chemical reactions. The system energy is divided into partial energy contributions, which include bonded and non-bonded terms[29]

$$E_{\text{system}} = E_{\text{bond}} + E_{\text{over}} + E_{\text{under}} + E_{\text{val}} + E_{\text{pen}} + E_{\text{tors}} + E_{\text{conj}} + E_{\text{vdWaals}} + E_{\text{coulomb}}, \quad (1)$$

where the energy terms are defined as bond energy (E_{bond}), over-coordination (E_{over}), under-coordination (E_{under}), valence energy (E_{val}), energy penalty for handling atoms with two double bonds (E_{pen}), torsion energy (E_{tors}), conjugated bond

[a] *Instituto de Física "Gleb Wataghin", Universidade Estadual de Campinas, 13083-970, Campinas, São Paulo, Brazil*
[b] *Departamento de Física, IGCE, Universidade Estadual Paulista, UNESP, 13506-900, Rio Claro, SP, Brazil. E-mail: paupitz@rc.unesp.br; Tel: +55-19-35269156*

† Electronic supplementary information (ESI) available: Videos showing the unzipping process and stress distributions. See DOI: 10.1039/c3cp52701h

energies (E_{conj}), van der Waals energy ($E_{vdWaals}$) and Coulomb energy ($E_{coulomb}$). In order to obtain the reactivity during the simulations, all bond orders are calculated, and charge effects are taken into account using the electronegativity equalization method (EEM) approach.[31,32] This is a powerful tool that makes it possible to carry out simulations of large systems, over long periods of time, describing the formation and breaking of chemical bonds.

3 Results

We have considered double-walled BNNTs of different chiralities (armchair, zigzag and chiral ones). The inner tube was kept fixed in order to mimic a rigid many layers core. In our simulations, the chirality of inner tubes showed no significant influence on the cracking patterns. Then, structural defects were created on the outer tube and this tube was subjected to an externally applied mechanical strain. This strain was generated by pulling a lateral band of atoms at a constant velocity of 10^{-3} Å fs^{-1}, until a structural failure, characterized by an abrubt local stress decrease (as the chemical bonds return to their equilibrium length), occurred (see Fig. 1). This mechanical failure is characterized by an abrupt decrease of the local stress values, as evidenced by the bond-length values returning to their equilibrium (non-stressed) values. We have also calculated the per atom von Mises stress.[33] The von Mises stress values provide a good estimate of the level of structural distortions of the system, which is very helpful in the analysis of fracture processes. This approach has been successfully used before in the analysis of the processes of CNT unzipping.[34]

In Fig. 2 we present the fracture patterns for the different tube chiralities. As we can see from this figure, the fracture patterns are significantly chirality dependent. Armchair BNNTs fracture parallel to their longitudinal axis, exposing extremely smooth zigzag edges. Once a fracture line is created it does not change direction during the whole unzipping process. These results suggest that armchair BNNTs might be very good candidates for producing high quality zigzag BN nanoribbons with well defined and smooth edges.

Chiral BNNTs on the other hand, tend to exhibit mostly zigzag edges. The fracture line changes directions erratically during the unzipping process, in general not following the tube longitudinal axis direction. The generated exposed edges are neither armchair nor zigzag ones.

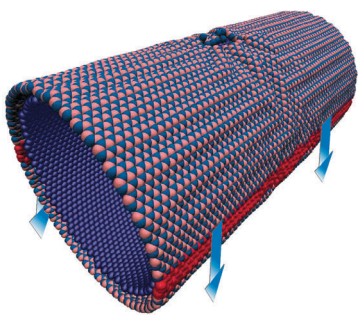

Fig. 1 Scheme of the atomistic model used in the molecular dynamics simulations. Defective external tube atoms are free to move. Inner tube atoms are held fixed. Lateral bands represent ''clamped'' atoms which are moved along the directions indicated by the arrows at constant velocity. See text for discussions.

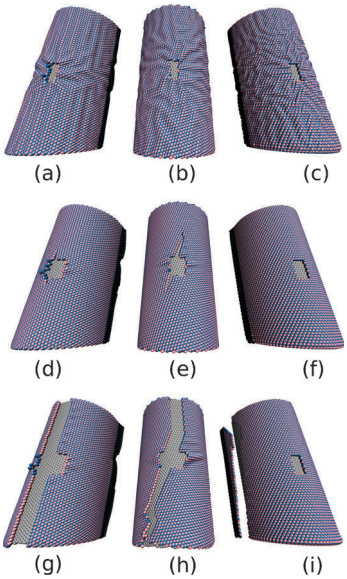

Fig. 2 Representative snapshots from the molecular dynamics simulations of the unzipping process for BNNTs with different chiralities. (a), (b) and (c) represent the unzipping initial stages, while (d), (e) and (f) are intermediate stages and (g), (h) and (i) are the advanced stages of unzipping for armchair, chiral and zigzag BNNTs, respectively. See text for discussions.

For the investigated cases of zigzag tubes the fractures occur even before the induced strain can propagate to the defective areas. Complete ruptures occur on both sides of the tubes, near the region of the band of pulled atoms. These results indicate that zigzag BNNTs exhibit an extremely limited capability of withstanding strain, and redistributing the mechanical stress. Also, the exposed edges are quite irregular, but with a predominance of armchair ones. These fracture pattern chirality dependences can be better evidenced in videos in the ESI.†

Our results suggest that armchair BNNTs are excellent candidates for producing high quality, smooth edged BN nanoribbons, but chiral and zigzag ones are not. However, the stress distributions (see Fig. 3 and 4) are surprisingly uniform for all tube chiralities. It should be stressed that the BNNT unzipping patterns are quite different to the ones presented by CNTs.[34]

These features can be understood by considering the fact that Boron nitride interlayer interactions are expected to play an important role in the mechanical properties of multi-walled BNNTs and nanosheets.[35–37] The B–N interactions cause a strong mechanical coupling between adjacent layers whose effect is two-fold: first, it increases the difficulty of adjacent layers to slip against each other, increasing the material stiffness; second, it avoids the fast redistribution of stress through the structure. This is exhibited more often in zigzag tubes, in which case most of the created strain cannot reach the defective region before the tube starts to crack. This strong mechanical coupling causes stress levels on the tubes to be typically one order of magnitude higher than those observed in the unzipping of CNTs.[34]

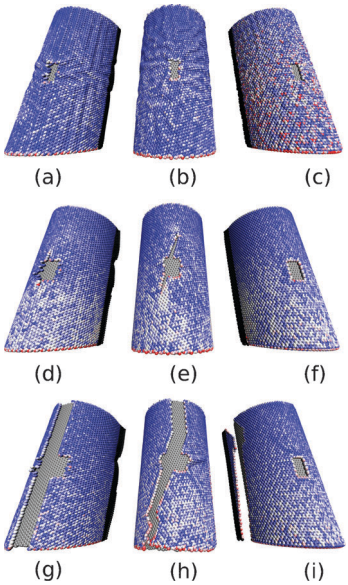

Fig. 3 Stress profile distribution for representative snapshots from the molecular dynamics simulations for the corresponding cases presented in Fig. 2. Results for armchair BNNTs: (a), (d) and (g). Chiral BNNT: (b), (e) and (h). Zigzag BNNTs: (c), (f) and (i). See text for discussions.

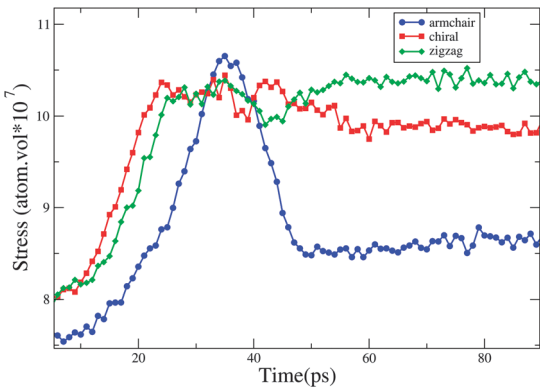

Fig. 4 Comparison of mean distortional stress (von Mises Stress) for different chirality tubes. Stress units are in atm × vol, vol being the atomic volume in accordance with LAMMPS protocols.[30]

We have also investigated the effects of the presence of extensive defects on the tube morphology (see Fig. 5). These simulations involve a large number of atoms (about 50 000 atoms), all of them free to move and in the absence of externally applied forces. The simulations were carried out at T = 300 K.

Similarly to what was observed in CNTs,[34] those defects create regions of high curvature and, consequently, of high chemical reactivity. When many of these defects are present (and close enough together), a deformed region connecting these defects is formed. When the defects are too far apart, only one high curvature area is formed (see Fig. 5). These results show that we will always have the formation of only one highly curved region on the BNNTs. As the curvature of these regions increases, the chemical reactivity is also significantly increased and, at the same time, a change in the character of BN bonds occurs in these regions, going from sp^2 to sp^3 hybridized states. As a consequence, a 'crest' region is formed, which works as a well-defined path to the bond-breaking unzipping processes. This might explain why only a few cutting lines are frequently experimentally observed in unzipped carbon and BN tubes. As the chemical and/or physical processes can generate multiple and simultaneously formed deffective areas, we could expect that each one of the areas could generate an unzipping path, but this is not observed. The 'crest' effect can explain this.

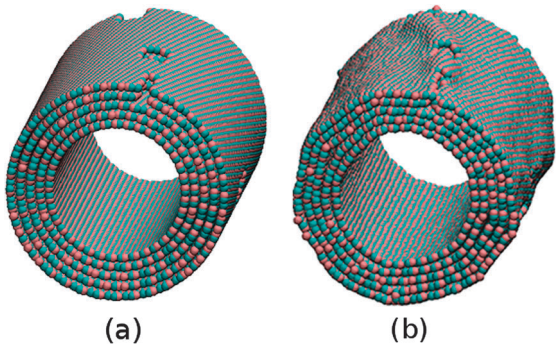

Fig. 5 Representative snapshots of defective tubes. (a) Initial configuration. (b) Final configuration, with the crest formed. See text for discussions.

4 Summary and conclusions

We have investigated, through reactive fully atomistic molecular dynamics simulations, the unzipping processes of boron nitride nanotubes (BNNTs) under mechanical stress. We have considered tubes of different diameters and chiralities. Our results showed that the chirality is of fundamental importance in defining the fracture patterns and the resulting topology of the formed unzipped structures. Only unzipped armchair BNNTs showed the formation of well defined zigzag BN nanoribbons. The BNNT unzipping patterns are quite different from the ones reported for CNTs under the same conditions.[34,38] This can be explained by the pronounced differences between adjacent tube coupling for the carbon and BN tubes.[37] We have also observed the formation of 'crest' (regions of high curvature) structures that might explain why only a few cut lines are observed for unzipped BNNTs.

Acknowledgements

This work was supported in part by the Brazilian Agencies CNPq and FAPESP. The authors thank the Center for Computational Engineering and Sciences at Unicamp for financial support through the FAPESP/CEPID Grant #2013/08293-7. RP also acknowledges FAPESP Grant #2011/17253-3.

References

1 K. S. Novoselov, A. K. Geim, S. V. Morozov, D. Jiang, Y. Zhang, S. V. Dubonos, I. V. Grigorieva and A. A. Firsov, *Science*, 2004, **306**, 666–669.
2 J. Li, C. Cao and H. Zhu, *Nanotechnology*, 2007, **18**, 115605.

3 D. C. Elias, R. R. Nair, T. M. G. Mohiuddin, S. V. Morozov, P. Blake, M. P. Halsall, A. C. Ferrari, D. W. Boukhvalov, M. I. Katsnelson, A. K. Geim and K. S. Novoselov, *Science*, 2009, **323**, 610–613.
4 R. H. Baughman, H. Eckhardt and M. Kertesz, *J. Chem. Phys.*, 1987, **87**, 6687–6699.
5 P. Vogt, P. De Padova, C. Quaresima, J. Avila, E. Frantzeskakis, M. C. Asensio, A. Resta, B. Ealet and G. Le Lay, *Phys. Rev. Lett.*, 2012, **108**, 155501.
6 C. Y. He, L. Z. Sun, C. X. Zhang, X. Y. Peng, K. W. Zhang and J. X. Zhong, *Phys. Chem. Chem. Phys.*, 2012, **14**, 10967–10971.
7 Y. K. E. Yap, *B–C–N Nanotubes and Related Nanostructures*, Heidelberg, Springer, 2009.
8 Y. Xie, H. T. Yu, H. X. Zhang and H. G. Fu, *Phys. Chem. Chem. Phys.*, 2012, **14**, 4391–4397.
9 C. Jin, F. Lin, K. Suenaga and S. Iijima, *Phys. Rev. Lett.*, 2009, **102**, 195505.
10 J. C. Meyer, A. Chuvilin, G. Algara-Siller, J. Biskupek and U. Kaiser, *Nano Lett.*, 2009, **9**, 2683–2689.
11 L. Song, L. Ci, H. Lu, P. B. Sorokin, C. Jin, J. Ni, A. G. Kvashnin, D. G. Kvashnin, J. Lou, B. I. Yakobson and P. M. Ajayan, *Nano Lett.*, 2010, **10**, 3209–3215.
12 H. Zeng, C. Zhi, Z. Zhang, X. Wei, X. Wang, W. Guo, Y. Bando and D. Golberg, *Nano Lett.*, 2010, **10**, 5049–5055.
13 X. Wang, C. Zhi, L. Li, H. Zeng, C. Li, M. Mitome, D. Golberg and Y. Bando, *Adv. Mater.*, 2011, **23**, 4072–4076.
14 C. Y. Zhi, Y. Bando, C. C. Tang, H. Kuwahara and D. Golberg, *Adv. Mater.*, 2009, **21**, 2889–2893.
15 E. Perim and D. S. Galvao, *Nanotechnology*, 2009, **20**, 335702.
16 X. Chen, R. A. Boulos, J. F. Dobson and C. L. Raston, *Nanoscale*, 2013, **5**, 498–502.
17 X. Li, X. Hao, M. Zhao, Y. Wu, J. Yang, Y. Tian and G. Qian, *Adv. Mater.*, 2013, **25**, 2200–2204.
18 L. Jiao, L. Zhang, X. Wang, G. Diankov and H. Dai, *Nature*, 2009, **458**, 877–880.
19 J. Zeng, K.-Q. Chen and C. Q. Sun, *Phys. Chem. Chem. Phys.*, 2012, **14**, 8032–8037.
20 S. Tang and Z. Cao, *Phys. Chem. Chem. Phys.*, 2010, **12**, 2313–2320.
21 L. Lai, J. Lu, L. Wang, G. Luo, J. Zhou, R. Qin, Z. Gao and W. N. Mei, *J. Phys. Chem. C*, 2009, **113**, 2273–2276.
22 F. Zheng, G. Zhou, Z. Liu, J. Wu, W. Duan, B. Gu and S. B. Zhang, *Phys. Rev. B: Condens. Matter Mater. Phys.*, 2008, **78**, 205415–205419.
23 C.-H. Park and S. G. Louie, *Nano Lett.*, 2008, **8**, 2200–2203.
24 V. Barone and J. E. Peralta, *Nano Lett.*, 2008, **8**, 2210–2214.
25 W. Chen, Y. Li, G. Yu, C.-Z. Li, S. B. Zhang, Z. Zhou and Z. Chen, *J. Am. Chem. Soc.*, 2010, **132**, 1699–1705.
26 D. V. Kosynkin, A. L. Higginbotham, A. Sinitskii, J. R. Lomeda, A. Dimiev, B. K. Price and J. M. Tour, *Nature*, 2009, **458**, 872–876.
27 J. L. Li, K. N. Kudin, M. J. McAllister, R. K. Prud'homme, I. A. Aksay and R. Car, *Phys. Rev. Lett.*, 2006, **96**, 176101.
28 K. J. Erickson, A. L. Gibb, A. Sinitskii, M. Rousseas, N. Alem, J. M. Tour and A. K. Zettl, *Nano Lett.*, 2011, **11**, 3221–3226.
29 A. C. T. van Duin, S. Dasgupta, F. Lorant and W. A. Goddard, *J. Phys. Chem. A*, 2001, **105**, 9396–9409.
30 S. Plimpton, *J. Comput. Phys.*, 1995, **117**, 1–19.
31 W. J. Mortier, S. K. Ghosh and S. Shankar, *J. Am. Chem. Soc.*, 1986, **108**, 4315–4320.
32 G. O. A. Janssens, B. G. Baekelandt, H. Toufar, W. J. Mortier and R. A. Schoonheydt, *J. Phys. Chem.*, 1995, **99**, 3251–3258.
33 A. Zang and O. Stephansson, *Stress field of the Earth's crust*, New York, Springer, 2010.
34 R. P. B. dos Santos, E. Perim, P. A. S. Autreto, G. Brunetto and D. S. Galvao, *Nanotechnology*, 2012, **23**, 465702.
35 J. Garel, I. Leven, C. Zhi, K. S. Nagapriya, R. Popovitz-Biro, D. Golberg, Y. Bando, O. Hod and E. Joselevich, *Nano Lett.*, 2012, **12**, 6347–6352.
36 D. Golberg, Y. Bando, Y. Huang, T. Terao, M. Mitome, C. Tang and C. Zhi, *ACS Nano*, 2010, **4**, 2979–2993.
37 N. Marom, J. Bernstein, J. Garel, A. Tkatchenko, E. Joselevich, L. Kronik and O. Hod, *Phys. Rev. Lett.*, 2010, **105**, 046801.
38 H. Zhang, M. Zhao, T. He, X. Zhang, Z. Wang, Z. Xi, S. Yan, X. Liu, Y. Xia and L. Mei, *Phys. Chem. Chem. Phys.*, 2010, **12**, 13674–13680.

